

# Nanoscale Advances

Accepted Manuscript

This article can be cited before page numbers have been issued, to do this please use: P. Zhao, J. Wei, F. Wang, Y. Luo and L. Yang, *Nanoscale Adv.*, 2025, DOI: 10.1039/D5NA00748H.



This is an Accepted Manuscript, which has been through the Royal Society of Chemistry peer review process and has been accepted for publication.

Accepted Manuscripts are published online shortly after acceptance, before technical editing, formatting and proof reading. Using this free service, authors can make their results available to the community, in citable form, before we publish the edited article. We will replace this Accepted Manuscript with the edited and formatted Advance Article as soon as it is available.

You can find more information about Accepted Manuscripts in the [Information for Authors](#).

Please note that technical editing may introduce minor changes to the text and/or graphics, which may alter content. The journal's standard [Terms & Conditions](#) and the [Ethical guidelines](#) still apply. In no event shall the Royal Society of Chemistry be held responsible for any errors or omissions in this Accepted Manuscript or any consequences arising from the use of any information it contains.

## ARTICLE

# Utilization of Waste Leather for Efficient Removal of $\text{Ca}^{2+}$ and $\text{Mg}^{2+}$ via Nano-structural Adsorption in Lithium Carbonate Production

Received 00th January 20xx,  
Accepted 00th January 20xx

DOI: 10.1039/x0xx00000x

Pengxiang Zhao<sup>a,\*</sup>, Jianyu Wei<sup>c</sup>, Fumei Wang<sup>d</sup>, Yang Luo<sup>b</sup>, Luming Yang<sup>a,\*</sup>

With the growth of electric vehicles (EVs), the demand for battery grade lithium carbonate ( $\text{Li}_2\text{CO}_3$ ) is increasing significantly. However, large part of the  $\text{Li}_2\text{CO}_3$  is industrial-grade which cannot be satisfied with the preparation of cathode, either ternary material or lithium iron phosphate ( $\text{Li}_2\text{CO}_3$  is one of the precursors for either ternary material or lithium iron phosphate). Traditional production involves converting industrial-grade lithium carbonate into  $\text{LiHCO}_3$  solution through carbonization by using  $\text{CO}_2$ . The insoluble impurities are removed by filtering followed by thermal decomposition to produce battery-grade  $\text{Li}_2\text{CO}_3$ . However,  $\text{Ca}^{2+}$  and  $\text{Mg}^{2+}$  are the most difficult impurities to remove due to the similar behavior with  $\text{Li}^+$ . This study evaluates using vegetable-aldehyde combination tanned leather to filter  $\text{Ca}^{2+}$  and magnesium  $\text{Mg}^{2+}$  ions from  $\text{LiHCO}_3$  solution via the nano structure of the leather. The results show effective reduction of  $\text{Ca}^{2+}$  and  $\text{Mg}^{2+}$  concentrations from  $\text{LiHCO}_3$  solution. Treated with EDTA, the leather can be reused for at least 12 cycles, that ensure the high-quality lithium carbonate production cost-effectively and sustainably. The study highlights the tanned leather's potential as a reliable filtration medium for lithium-ion battery precursors.

**Keywords:** electric vehicles; industrial grade lithium carbonate; battery grade lithium carbonate; tanned leather; sustainability

## 1 Introduction

Battery-grade lithium carbonate ( $\text{Li}_2\text{CO}_3$ ) is an irreplaceable compound used as a precursor for cathode materials in lithium-ion batteries.<sup>1,2</sup> With the growth of electric vehicles (EVs), the demand for battery grade lithium carbonate ( $\text{Li}_2\text{CO}_3$ ) is increasing significantly. As the primary precursor for lithium-ion battery cathodes, battery-grade lithium carbonate plays a crucial role in battery performance and safety.<sup>3-5</sup> With increasing concerns regarding the safety of lithium-ion batteries, the focus within the lithium chemical industry has shifted toward improving battery safety and reducing impurity levels in

cathode materials and their precursors.<sup>6</sup>

Currently, the most common method for producing battery-grade lithium carbonate involves converting industrial-grade or crude lithium carbonate into  $\text{LiHCO}_3$  solution by introducing  $\text{CO}_2$ .<sup>7,8</sup> After filtration, the  $\text{LiHCO}_3$  solution undergoes thermal decomposition to produce  $\text{Li}_2\text{CO}_3$ , which is then subjected to centrifugation, washing, and drying to yield the final product.<sup>9</sup> In this process, the removal of  $\text{Ca}^{2+}$  and magnesium  $\text{Mg}^{2+}$  impurities is typically achieved through a two-step procedure.<sup>10</sup> The first step involves filtering the  $\text{LiHCO}_3$  solution to remove most of the insoluble  $\text{Ca}^{2+}$  and  $\text{Mg}^{2+}$  precipitates.<sup>11</sup> The second step employs ion exchange resins, filtration membranes, or chelating agents to deeply purify the filtered  $\text{LiHCO}_3$  solution by removing residual  $\text{Ca}^{2+}$  and  $\text{Mg}^{2+}$  ions.<sup>12</sup>

Grágeda<sup>13</sup> uses a combination of chemical precipitation and ion exchange technologies to remove major impurities from natural brine: calcium, magnesium, and sulfates. The results show that the combined use of chemical precipitation and ion exchange resins can achieve removal efficiencies as high as 99.93% (for magnesium), 98.93% (for calcium), and 97.14% (for sulfates). Additionally, Chen<sup>14</sup> added sodium carbonate to the sulfate solution to precipitate lithium carbonate ( $\text{Li}_2\text{CO}_3$ ). Then, lithium carbonate was put into water to prepare lithium carbonate slurry, and  $\text{CO}_2$  was added to it.

<sup>a</sup> National Engineering Laboratory for Clean Technology of Leather Manufacture, Sichuan University, Chengdu, China, 610000 Email: ylm11982@126.com

<sup>b</sup> GUANGZHOU SHILING LEATHER GOODS INDUSTRY RESEARCH CENTER CO.,LTD. Guangzhou, China, 510800.

<sup>c</sup> School of Materials and New Energy, Ningxia University, Yinchuan, Ningxia 750021, China

<sup>d</sup> School of Materials Science and Engineering, Xihua University, Chengdu 610039, China

† Footnotes relating to the title and/or authors should appear here.

Supplementary Information available: [details of any supplementary information available should be included here]. See DOI: 10.1039/x0xx00000x



Subsequently, Dowex G 26 resin was used to remove calcium and sodium from lithium carbonate. Milyutin<sup>15</sup> uses inorganic adsorbent and organic ion exchange resin to remove alkaline earth metal and nonferrous metal ions, thus obtaining high purity lithium carbonate. However, each of these methods in the second step has its advantages and disadvantages: i) Ion exchange resins effectively remove divalent  $\text{Ca}^{2+}$  and  $\text{Mg}^{2+}$  ions, but can produce large amounts of waste acid, which is environmentally unfriendly. ii) Membrane filtration is efficient but costly, and the precipitation of lithium carbonate in the  $\text{LiHCO}_3$  solution can cause blockages. iii) Chelating agents effectively sequester  $\text{Ca}^{2+}$  and  $\text{Mg}^{2+}$  ions, but their introduction into the mother liquor can disrupt the recycling of the lithium carbonate solution.<sup>16,17</sup> Additionally, most chelating agents contain nitrogen, which can impart an unpleasant odor to the lithium carbonate product. Thus, developing an environmentally friendly and efficient process for the removal of  $\text{Ca}^{2+}$  and  $\text{Mg}^{2+}$  impurities from battery-grade lithium carbonate is of significant importance.

It is known that leather is primarily composed of collagen, which contains a high density of carboxyl ( $-\text{COOH}$ ) and amino ( $-\text{NH}_2$ ) groups.<sup>18–20</sup> The leather goods industry generates substantial amounts of leather waste, mainly as by-products from production processes.<sup>21</sup> Utilizing the carboxyl and amino groups in these leather wastes to adsorb  $\text{Ca}^{2+}$  and  $\text{Mg}^{2+}$  ions from the  $\text{LiHCO}_3$  solution not only holds potential for improving the removal of impurities in lithium carbonate production, but also offers an effective means of recycling leather waste, thereby reducing environmental pollution.<sup>22</sup>

In mechanistic aspect, the native carboxyl ( $-\text{COOH}$ ) and amino ( $-\text{NH}_2$ ) groups present on the molecular chains of both leather collagen and tanning agents are its core adsorption mechanism. These functional groups can efficiently and selectively adsorb and remove divalent metal ions, such as calcium ( $\text{Ca}^{2+}$ ) and magnesium ( $\text{Mg}^{2+}$ ), from the solution through electrostatic attraction and complexation.

In this study, the feasibility of using leather waste for the removal of calcium and magnesium ions is demonstrated. Indeed, this study investigated the performance of leather tanned with different tanning agents in removing calcium and magnesium ions from  $\text{LiHCO}_3$  solution, and subsequently conducted their recycling tests of calcium and magnesium ions removal.

## 2 Experimental sections

### 2.1 Materials

The plant tannins (Black Wattle Extract) that used for plant tanning were supplied by Jiangxi Gannan Heijingshu Castanopsis Factory. For the aldehyde tanning, glutaraldehyde was purchased from Sigma-Aldrich (USA). The combined plant-aldehyde tanning process utilized a mixture of the previously mentioned plant tannins and glutaraldehyde. Additionally, the goatskins used for tanning were sourced from a local supplier. Other chemicals and solvents required for the process, including formic acid and sodium bicarbonate, were obtained from Sigma-Aldrich (USA) and used without further purification. The original material of this verification

is commercial industrial-grade lithium carbonate (purchased from Sichuan Guangxing Lithium Battery Technology Co., Ltd.)

### 2.2 Operation process

The preparation of tanned goatskins is divided into three types : i) plant tanning ; ii) aldehyde tanning ; iii) combined plant-aldehyde tanning. The details of the preparation are in Supporting Information. As illustrated in Figure 1, the use of leather as a filter paper for removing calcium and magnesium ions from a lithium bicarbonate solution follow several steps. i) Place a standard piece of filter paper as first filter layer (approximately 7 cm in diameter) at the bottom of a Buchner funnel; ii) place a piece of leather as second filter layer (approximately 7 cm in diameter) on top of the filter paper inside the Büchner funnel; iii) pour 2000 ml lithium bicarbonate solution (with the concentration of  $\text{Li}_2\text{O}$  20g/L) into the Büchner funnel; iv) the solution passes through the sheepskin and filter paper, effectively filtering out the calcium and magnesium ions.

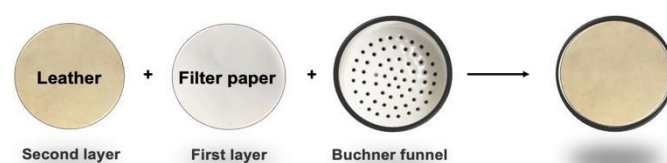


**Figure 1** The schedule of using leather as filter medium to remove  $\text{Ca}^{2+}$  and  $\text{Mg}^{2+}$  from a lithium bicarbonate solution.

### 2.3 Characterization

The FT-IR spectra of the tanned leather samples were recorded using a Perkin-Elmer Spectrum-One spectrophotometer. The samples were prepared by mixing 1 wt% tannin with KBr and pressing into pellets. The spectra were collected in the range of 4000 to 450  $\text{cm}^{-1}$  with 32 scans and a resolution of 4  $\text{cm}^{-1}$ . The mechanical properties, including stress and toughness, of the tanned leather samples were measured using a universal testing machine (Instron). The samples were cut into standard dumbbell shapes, and the tensile tests were performed at a crosshead speed of 10 mm/min until failure. The stress and toughness values were calculated from the stress-strain curves. The shrinkage temperature ( $T_s$ ) of the tanned leather samples was determined using a shrinkage tester (SATRA TM 31). The samples were heated at a constant rate, and the temperature at which the leather started to shrink was recorded as the  $T_s$  value. X-ray photoelectron spectroscopy (XPS) was performed using a Kratos Axis Ultra DLD spectrometer with a monochromatic Al  $K\alpha$  source (1486.6 eV). The spectra were collected at a pass energy of 160 eV for survey scans and 40 eV for high-resolution scans. The surface composition and chemical states of the elements present in the leather samples were analyzed. Scanning electron microscopy (SEM) was conducted using a JEOL JSM- 6510LV microscope. The leather samples were sputter-coated with a thin layer of gold to enhance conductivity. The microstructure of the tanned leather was observed at various magnifications to assess the fiber network and morphology. The isoelectric point of the tanned leather samples was determined by measuring the zeta potential as a function of pH using a zeta potential analyzer (Malvern Zetasizer Nano ZS). The samples were dispersed in water, and the pH was adjusted using hydrochloric acid (HCl) and sodium hydroxide (NaOH) solutions. The pH at which the zeta potential reached zero was recorded as the isoelectric point. The concentration of calcium and magnesium impurity ions is



determined by ICP (Inductively Coupled Plasma). The ICP process involves nebulizing the solution to form an aerosol that is introduced into the plasma flame, causing the atoms and ions in the solution to become excited. Then, the energy spectral lines and intensities of the excited particles as they transition back to the ground state are measured, thereby determining the content of elements in the product.

## 2.4 Computational Details

The Density functional theory (DFT) calculations were conducted using the ADF2023 program. The hybrid B3LYP functional was employed in conjunction with an all-electron triple- $\zeta$  Slater basis set, augmented by two polarization functions (STO-TZ2P). To account for dispersion forces, Grimme's DFT-D3(BJ) corrections were applied. The bonding energy ( $E_{\text{bond}}$ ) between the metal cation ( $M^{2+}$ ,  $M = \text{Mg, Ca}$ ) and the chelating ligands ( $L^{2-}$ ) is obtained by using the following equation:

$$E_{\text{bond}} = E(\text{ML}) - E(M^{2+}) - E(L^{2-}) \quad (1)$$

## 3 Results and discussion

### 3.1 Material Characterization of Goat Skin Before and After Tanning

The stress, toughness and maximum stress temperature of goat skin before and after tanning well characterized (see Figure S1-S3). Particularly, by comparing the infrared spectra before and after tanning, key absorption bands that correspond to different chemical groups are observed. Among these, the amide I (around  $1650 \text{ cm}^{-1}$ ), amide II (around  $1550 \text{ cm}^{-1}$ ), and amide III (around  $1250 \text{ cm}^{-1}$ ) bands are related to amide groups<sup>23</sup>. By analyzing the spectra of different tanning processes (the black line represents raw goat skin, the red line represents TWS, the blue line represents vegetable tanning, and the green line represents vegetable-aldehyde combination tanning), we can observe changes in these characteristic absorption bands.

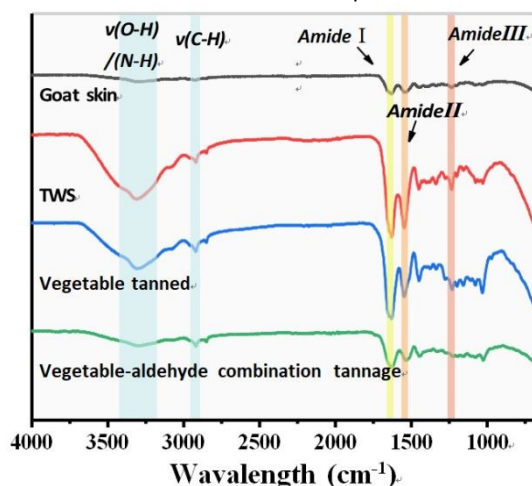


**Figure 2** Infrared spectra comparison of different types of leather. (Black line: raw goat skin; red line: TWS tanning; blue line: vegetable tanning; green line: vegetable-aldehyde combination tanning).

It is obvious that the tanning process increases the amide groups, the intensity of the amide I, amide II, and amide III bands will be significantly stronger in the tanned samples (red, blue, and green lines). In the spectra, the absorption intensity at  $1650 \text{ cm}^{-1}$ ,  $1550 \text{ cm}^{-1}$ , and  $1250 \text{ cm}^{-1}$  is indeed higher for the red, blue, and green lines compared to the black line. This indicates that the tanning process introduces more amide groups due to the presence of amide groups in tanned agent, and subsequently increasing the intensity of these absorption bands. Thus, comparing the infrared spectra before and after tanning shows that the tanning process indeed increases the number of amide groups in the sample. This is likely due to the formation of new amide bonds between collagen fibers and tanning agents during the tanning process.

In addition, the XPS analysis of goat skin before and after tanning was also conducted (see Figure S4-S7). Particularly, the following four graphs in Figure 3 provide valuable insights into the chemical composition and bonding environment of the goat leather samples before and after treatment. For the goat skin without tanning (Figure 3a), the O 1s spectrum shows two main components: C-O (purple) and C=O (orange). This indicates the presence of both single and double bonded oxygen atoms, suggesting a relatively balanced mixture of these functional groups. However, for those tanned leather, including TWS tanned (Figure 3b), vegetable tanned (Figure 3c), and vegetable-aldehyde combination tanned (Figure 3d), show noticeable increases in the C=O component. The results indicate that different tanning processes have various effects on the chemical composition of goat leather, particularly in the formation of carbonyl groups (C=O). The combination of vegetable and acid tanning appears to be the most effective method for enhancing these functional groups in the leather.

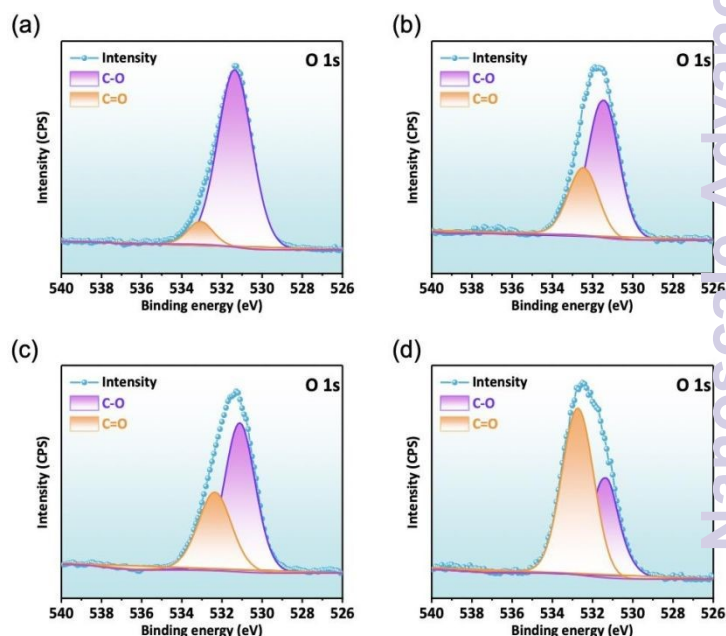


**Figure 3** XPS of C=O bond in different types of leather. (a: raw goat skin; b: TWS tanning; c: vegetable tanning; d: vegetable-aldehyde combination tanning).



Besides, compared with the un-tanned goat skin (Figure 4a) the chemicals used react with the collagen fibers in the tanned leather to form a stable cross-linked structure (See Figure 4 b, c and d). This structural change can be observed in SEM images, which show densely packed fibers and fewer pores.

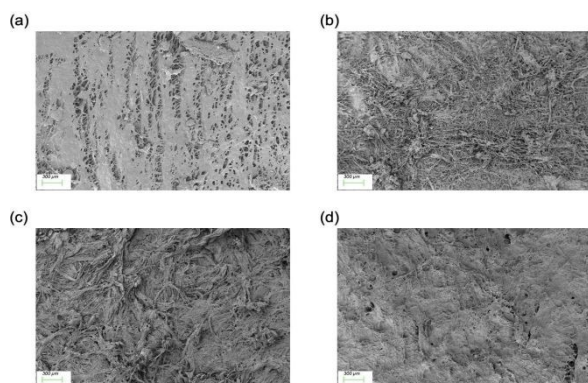


**Figure 4** SEM of Microstructure of different types of leather. (a: raw goat skin; b: TWS tanning; c: vegetable tanning; d: vegetable-aldehyde combination tanning).

In summary, the enrichment of amide functional groups (Figure 3) and the changes in the fiber nanoscale structure of the leather after tanning (see figure 4) suggest that the tanned leather may have the potential to adsorb calcium and magnesium ions from the solution through coordination and physical adsorption. Specifically, the tanning process increases the number of amide groups in the leather, and these functional groups can form stable coordination bonds with calcium and magnesium ions. Additionally, the tanned leather becomes compact and dense, increasing its surface area, which enables more efficient physical adsorption. Together, these factors may enhance the ability of the tanned leather to adsorb calcium and magnesium ions from solutions.

### 3.2 Removal of $\text{Ca}^{2+}$ and $\text{Mg}^{2+}$ by using untanned and tanned leather

Typically, battery-grade lithium carbonate requires calcium and magnesium ions to be within 50 ppm. This means that in a lithium bicarbonate solution with an  $\text{Li}_2\text{O}$  concentration of 20 g/L, the content of calcium and magnesium should be less than 2.5 mg/L, which is less than 2.5 mg/L. The removal performance of  $\text{Ca}^{2+}$  and  $\text{Mg}^{2+}$  in  $\text{LiHCO}_3$  solution is conducted as illustrated in in Figure 1. As indicated in Table 1, different types of leather filters were tested for removing  $\text{Ca}^{2+}$  and  $\text{Mg}^{2+}$  ions from lithium bicarbonate solution. The results showed that raw goat skin slightly reduced ion concentrations, while TWS tanned leather and vegetable tanned leather both brought the levels down to within acceptable limits. However, the most effective was the vegetable-aldehyde combination tanned leather, which significantly reduced the ion concentrations to well below the required threshold of 2.5 mg/L for battery-grade lithium carbonate.

**Table 1** The removal of  $\text{Ca}^{2+}$  and  $\text{Mg}^{2+}$  in  $\text{LiHCO}_3$  solution by different types of leather.

Samples	$\text{Ca}^{2+}$ (mg/L)	$\text{Mg}^{2+}$ (mg/L)
Lithium bicarbonate solution (LBS)	7.5	4
LBS filter by raw goat skin	5.5	3.7
LBS filter by TWS tanned leather	2.5	2.2
LBS filter by vegetable tanned leather	2.4	2.1
LBS filter by vegetable-aldehyde combination tanned leather	1.7	1.2

Two main reasons could explain the results: i) the tanning process increases amide groups in leather, creating stable bonds with calcium and magnesium ions. The compact and the nano structure enhances surface area, improving physical adsorption and overall efficiency in adsorbing these ions from solutions. Thus, the tanned leather could reduce the ion concentration after filtration. ii) From the perspective of the isoelectric point (IP), leather's ability to filter  $\text{Ca}^{2+}$  and  $\text{Mg}^{2+}$  depends on the surface charge of the leather. In general, the leather's surface charge is neutral near the IP, leading to low adsorption of these ions. However, when the pH deviates from the IP, the leather surface gains a net charge, enhancing its ability to attract and adsorb oppositely charged ions like  $\text{Ca}^{2+}$  and  $\text{Mg}^{2+}$ . As shown in Figure 5, vegetable-aldehyde combination tanned leathers exhibit superior adsorption performance of  $\text{Ca}^{2+}$  and  $\text{Mg}^{2+}$ , which may be contributed to their IP that is far from the pH of  $\text{LiHCO}_3$  solution. In detail, the leather's superior performance is attributed to its low isoelectric point (IP) of 2.97, which is far from the  $\text{LiHCO}_3$  solution's pH of 9-10. This significant pH difference causes the leather's surface to become strongly negatively charged, creating a powerful electrostatic force that efficiently attracts and captures the positively charged  $\text{Ca}^{2+}$  and  $\text{Mg}^{2+}$  ions. This makes the leather a reliable and sustainable filtration medium for producing high-quality lithium carbonate.

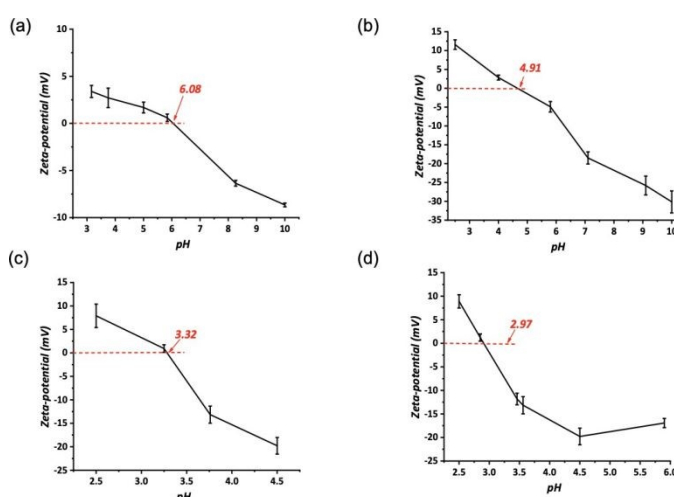


**Figure 5** Zeta position of in different types of leather. (a: raw goat skin; b: TWS tanning; c: vegetable tanning; d: vegetable-aldehyde combination tanning).

### 3.3 The removal amounts of $\text{Ca}^{2+}$ and $\text{Mg}^{2+}$ by using vegetable-aldehyde combination tanned leather



As mentioned above, each vegetable-aldehyde combination tanned leather is approximately 7 cm in diameter. In order to evaluate the efficacy of  $\text{Ca}^{2+}$  and  $\text{Mg}^{2+}$  performance, the amounts of  $\text{LiHCO}_3$ , with the concentration of 7.5 mg/L  $\text{Ca}^{2+}$  and  $\text{Mg}^{2+}$  4 mg/L, were varied, and the removal amounts of  $\text{Ca}^{2+}$  and  $\text{Mg}^{2+}$  were measured. From the table, it can be observed that with increasing amounts of  $\text{LiHCO}_3$  solution, the removal amounts of  $\text{Ca}^{2+}$  and  $\text{Mg}^{2+}$  by the vegetable-aldehyde combination tanned leather also increase. Initially, for 1L of  $\text{LiHCO}_3$  solution, the residual concentrations of  $\text{Ca}^{2+}$  and  $\text{Mg}^{2+}$  are 1.7 mg/L and 1.2 mg/L, respectively. As the volume of  $\text{LiHCO}_3$  solution increases to 30L, the residual concentrations rise to 2.4 mg/L for  $\text{Ca}^{2+}$  and 2.3 mg/L for  $\text{Mg}^{2+}$ .

However, as illustrated above, it is important to note that when the concentrations of  $\text{Ca}^{2+}$  and  $\text{Mg}^{2+}$  exceed 2.5 mg/L, the subsequent thermal decomposition of  $\text{LiHCO}_3$  into  $\text{Li}_2\text{CO}_3$  results in the impurities of  $\text{Ca}^{2+}$  and  $\text{Mg}^{2+}$  in the product exceeding acceptable standards. Therefore, treating up to 20 L of  $\text{LiHCO}_3$  is considered the safe range for removing  $\text{Ca}^{2+}$  and  $\text{Mg}^{2+}$  using 7 cm diameter vegetable-aldehyde combination tanned leather. This indicates that the vegetable-aldehyde combination tanned leather with diameter 7 cm is effective and safe for removing  $\text{Ca}^{2+}$  and  $\text{Mg}^{2+}$  when the volume of  $\text{LiHCO}_3$  solution does not exceed 20 L.

**Table 2** The residual concentration of  $\text{Ca}^{2+}$  and  $\text{Mg}^{2+}$  in  $\text{LiHCO}_3$  solution after filtration by vegetable-aldehyde combination tanned leather.

The amounts of $\text{LiHCO}_3$ solution	$\text{Ca}^{2+}$ (mg/L)	$\text{Mg}^{2+}$ (mg/L)
1L	1.7	1.2
5L	1.7	1.3
10L	1.9	1.5
20L	2.1	2.0
30L	2.4	2.5

### 3.4 DFT calculations

In order to reuse the tanned leather, the binding of  $\text{Ca}^{2+}$  and  $\text{Mg}^{2+}$  should be removed from the tanned leather. Thus, the chelating ligands, including EDTA, citrate, and tartrate, are considered.

As shown in Figure 6, the bonding energies between the metal cations ( $\text{Mg}^{2+}$ ,  $\text{Ca}^{2+}$ ) and the single chelating ligands (EDTA, citrate, and tartrate) were further investigated using DFT calculations. To ensure comparable charge states of the chelating complexes, the deprotonated forms of EDTA ( $[\text{C}_{10}\text{H}_{14}\text{N}_2\text{O}_8]^{2-}$ ), citrate ( $[\text{C}_6\text{H}_5\text{O}_7]^{2-}$ ), and tartrate ( $[\text{C}_4\text{H}_4\text{O}_6]^{2-}$ ) di-anions were used in the calculations. For the Mg series, the EDTA-Mg complex exhibits the lowest bonding energy (-698.36 kcal/mol), which is 67.82 kcal/mol and 75.31 kcal/mol lower than those of the citrate-Mg (-630.54 kcal/mol) and tartrate-Mg (-623.05 kcal/mol) complexes, respectively. A similar trend was observed for the Ca series, where the bonding energy of the EDTA-Ca complex (-597.28 kcal/mol) is significantly lower than those calculated for the citrate-Ca (-550.12 kcal/mol) and tartrate-Ca (-557.56 kcal/mol) complexes. These results indicate that, compared to citrate and tartrate, the EDTA ligand has a higher ability to chelate with  $\text{Mg}^{2+}$  and  $\text{Ca}^{2+}$  cations. Hence, the EDTA are used for remove the binding of  $\text{Ca}^{2+}$  and  $\text{Mg}^{2+}$  inside the tanned leather.

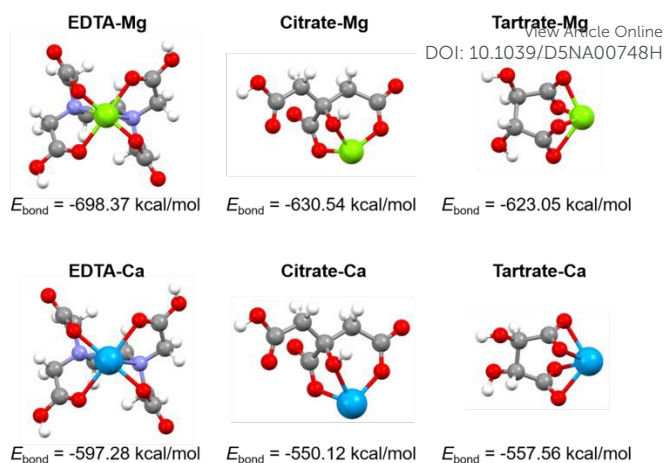


**Figure 6** DFT optimized structures of the magnesium and calcium chelates. The green ball, cyan ball, dark blue ball, red ball, grey ball and white ball represent Mg, Ca, N, O, C and H atoms, respectively.

### 3.5 The re-use of vegetable-aldehyde combination tanned leather

As shown in Figure 7, the vegetable-aldehyde combination tanned leather can be reused at least 12 times after enrichment with calcium and magnesium. By treating the leather with an EDTA solution, leveraging EDTA's strong binding ability with calcium and magnesium, the leather can be regenerated for continued use. Figure 6 illustrates the cyclic reuse of vegetable-aldehyde combination tanned leather. The figure shows the concentration changes of calcium ions ( $\text{Ca}^{2+}$ ) and magnesium ions ( $\text{Mg}^{2+}$ ) after 14 reuse cycles. It can be observed that, during the first 12 reuse cycles, the concentration of calcium and magnesium ions remains relatively stable between 2.1 mg/L to 2.3 mg/L, indicating that the leather can be reused at least 12 times. Also, the infrared spectrum in Figure S8 proved the existence of hydroxyl and amino functional groups still exist.

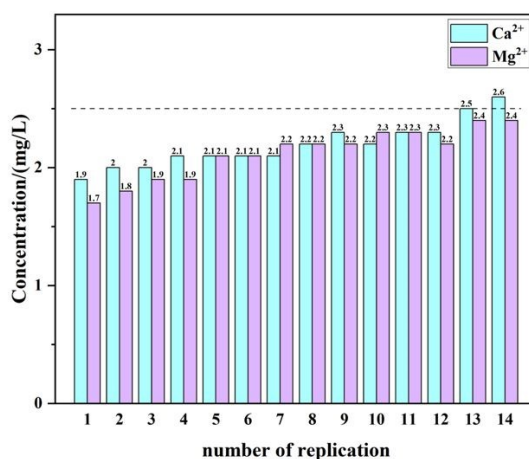


**Figure 7** The recycling of vegetable-aldehyde combination tanned leather for removal  $\text{Ca}^{2+}$  and  $\text{Mg}^{2+}$ .

### Conclusions



In conclusion, this article evaluated the efficacy of using vegetable-aldehyde combination tanned leather as a filter medium to remove calcium  $\text{Ca}^{2+}$  and magnesium  $\text{Mg}^{2+}$  ions from lithium bicarbonate  $\text{LiHCO}_3$  solution. The results demonstrated that the vegetable-aldehyde combination tanned leather is highly effective in reducing the concentrations of  $\text{Ca}^{2+}$  and  $\text{Mg}^{2+}$ . Additionally, the used leather can be treated with EDTA solution to chelate and remove the absorbed  $\text{Ca}^{2+}$  and  $\text{Mg}^{2+}$  ions, allowing the leather to be reused at least 12 times. This study found that the leather can be effectively reused up to at least 12 times, making it a cost-effective and sustainable option. Overall, this study highlights the potential of vegetable-aldehyde combination tanned leather as a reliable and safe filtration medium for removing  $\text{Ca}^{2+}$  and  $\text{Mg}^{2+}$  ions from  $\text{LiHCO}_3$  solutions, ensuring the production of high-quality lithium carbonate. Last but not least, the reusability of the tanned leather further enhances its applicability and efficiency, presenting promising prospects for resource utilization and new energy industry applications.

## Acknowledgements

The funding of post-doc from Guangzhou and Leather and Leather Goods Industry Research Center and the funding from Aba science and technology bureau (item number: R22ZYF0003) are gratefully acknowledged.

## Notes and references

† Footnotes relating to the main text should appear here. These might include comments relevant not central to the matter under discussion, limited experimental and spectral data, and crystallographic data.

- [1] Yuan ZX, Jiang Y, Lin B, Chen W, Wang CY, Ding M and Li ZJ, Research progress of ion-initiated in situ generated solid polymer electrolytes for high-safety lithium batteries, *Acta Chimica Sinica*, **2023**, *81*, 1064–1080.
- [2] Wu CF, Wang C, Lu JJ, Yuan J, Zhu P and Wang Y, Crystallization of battery-grade lithium carbonate with high recovery rate via solid-liquid reaction, *Particuology*, **2024**, *92*, 95–105.
- [3] Torres WR, Nieto CHD, PrévotEAU A, Rabaey K and Flexer V, Lithium carbonate recovery from brines using membrane electrolysis, *J. Membr. Sci.*, **2020**, *615*, 118416.
- [4] Sun ZH, Chen Y, Wang CX, Hu WX, Sun ZJ, Shi J and Yang HY, Corrosion behavior of cobalt oxide and lithium carbonate on mullite-cordierite saggar used for lithium battery cathode material sintering, *Materials*, **2023**, *16*, 653.
- [5] Rosso L, Alcaraz L, Rodríguez-Largo O and López FA, Purification of  $\text{Li}_2\text{CO}_3$  obtained through pyrometallurgical treatment of NMC black mass from electric vehicle batteries, *ChemSusChem*, **2024**, e202401722.
- [6] Battistel A, Palagonia MS, Brogioli D, La Mantia F and Trócoli R, Electrochemical methods for lithium recovery: a comprehensive and critical review, *Adv. Mater.*, **2020**, *32*, 1905440.
- [7] Xu ZG and Sun SY, Preparation of battery-grade lithium carbonate with lithium-containing desorption solution, *Metals*, **2021**, *11*, 1490.
- [8] Wang S, Li JX, Liu HZ, Deng H, Chen HL, Sun SH, Chen HY and Yang H, Preparation of lithium carbonate by microwave assisted pyrolysis, *Chin. J. Chem. Eng.*, **2022**, *52*, 146–153.

[9] Lu JJ, Wu CF, Wang Y, Yuan J and Zhu P, Preparation of battery-grade lithium carbonate by microbubble enhanced  $\text{CO}_2$  gas-liquid reactive crystallization, *Green Chem.*, **2022**, *24*, 9084–9093.

[10] Xu WH, Liu DF, He LH and Zhao ZW, A comprehensive membrane process for preparing lithium carbonate from high Mg/Li brine, *Membranes*, **2020**, *10*, 371.

[11] Scrosati B and Garche J, Lithium batteries: Status, prospects and future, *J. Power Sources*, **2010**, *195*, 2419–2430.

[12] Quintero C, O'Brien S, Jeldres RI, Parada P, Flores L, Cortes R, Zuniga A and Grageda M, Development of a co-precipitation process for the preparation of magnesium hydroxide containing lithium carbonate from Li-enriched brines, *Hydrometallurgy*, **2020**, *198*, 105515.

[13] Grágeda M, González A, Grágeda M and Ushak S, Purification of brines by chemical precipitation and ion-exchange processes for obtaining battery-grade lithium compounds, *Int. J. Energy Res.*, **2018**, *42*, 2386–2399.

[14] Chen WS, Lee CH and Ho HJ, Purification of lithium carbonate from sulphate solutions through hydrogenation using the Dowex G26 resin, *Appl. Sci.*, **2018**, *8*, 2252.

[15] Milyutin VV, Nekrasova NA, Rudskikh VV and Volkova TS, Preparation of high-purity lithium carbonate using complexing ion-exchange resins, *Russ. J. Appl. Chem.*, **2020**, *93*, 549–553.

[16] Zhou M, Preparation of battery grade  $\text{Li}_2\text{CO}_3$  from defective product by the carbonation-decomposition method, *Cryst. Res. Technol.*, **2023**, *58*, 2200112.

[17] Xu ZH, Yu P, Liu Z, Li ZQ, Zhang F, Yu JC and Zhou R, Systemic and direct production of battery-grade lithium carbonate from a saline lake, *Ind. Eng. Chem. Res.*, **2014**, *53*, 16502–16507.

[18] Yang F, Zeng YW, Long YL, Ding HX and Li N, Research recap of membrane technology for tannery wastewater treatment: a review, *Collagen Leather*, **2023**, *5*, 132.

[19] Muthukrishnan L, Nanotechnology for cleaner leather production: a review, *Environ. Chem. Lett.*, **2021**, *19*, 2527–2549.

[20] Muralidharan V, Palanivel S and Balaraman M, Turning problem into possibility: A comprehensive review on leather solid waste intra-valorization attempts for leather processing, *J. Clean. Prod.*, **2022**, *367*, 133021.

[21] Ma JZ, Yang N, Shi JB and Yang XY, Tailoring the structure of layered double oxide for enhancing adsorption of anionic chemicals on collagen fibers in chrome-free leather processing, *Clean Technol. Environ. Policy*, **2022**, *24*, 2947–2955.

[22] Ayele M, Worku K, Ayele A, Adewumi O, Mengesha A, Ayele S and Abebe A, A review on utilization routes of the leather industry biomass, *Adv. Mater. Sci. Eng.*, **2021**, *2021*, 1503524.

[23] Narayanan P and Janardhanan SK, An approach towards identification of leather from leather-like polymeric material using FTIR-ATR technique, *Collagen Leather*, **2024**, *6*, 145.



All data supporting the findings of this study are available within the article and its Supplementary Information files.

[View Article Online](#)  
DOI: 10.1039/D5NA00748H